

A pressure-polishing set-up to fabricate patch pipettes that seal on virtually any membrane, yielding low access resistance and efficient intracellular perfusion

Mascia Benedusi · Marco Aquila · Alberto Milani ·
Giorgio Rispoli

Received: 27 February 2011 / Revised: 15 June 2011 / Accepted: 22 June 2011 / Published online: 15 July 2011
© European Biophysical Societies' Association 2011

Abstract When performing whole-cell configuration recordings, it is important to minimize series resistance to reduce the time constant of charging the cell membrane capacitance and to reduce error in membrane potential control. To this end, an existing method was improved by widening the patch pipette shank through the calibrated combination of heat and air pressure. The heat was produced by passing current through a filament that was shaped appropriately to ensure a homogeneous heating of the pipette shank. Pressurized air was applied to the lumen of a pipette, pulled from a borosilicate glass microcap, via the pressure port of a modified commercial holder. The pipette reshaping was viewed on an LCD monitor connected to a contrast-intensified CCD camera and coupled to a modified bright-field stereomicroscope. By appropriately regulating the timing of air pressure and the application of heating, the pipette shank and, independently, the tip opening diameter were widened as desired. The methods illustrated here to fabricate and use the patch pipettes, using just one glass type, allowed the sealing of a wide variety of cell types isolated from different amphibian, reptilian, fish, and mammalian tissues as well as a variety of artificial membranes made with many different lipid mixtures. The access resistance yielded by pressure-polished pipettes was approximately one-fourth the size of the one attained with conventional pipettes; besides improving

the electrical recordings, this minimized intracellular ion accumulation or depletion as well. Enlarged shank geometry allowed for fast intracellular perfusion as shown by fluorescence imaging, also via pulled quartz or plastic tubes, which could be inserted very close to the pipette tip.

Keywords Electrophysiology · Voltage clamp · Patch clamp · Whole cell · Rod outer segment

Introduction

Patch-clamp recording, developed in the late 1970s to directly observe single ion channel currents, has rapidly become the most important experimental tool to precisely measure plasma and intracellular membrane electrical properties. The technique has prompted an extraordinary knowledge advancement in fields as diverse as cell signaling, hormone secretion, structure-function relationships of membrane proteins, nuclear membrane trafficking, neuronal networks, and neuronal information storage (Sakmann and Neher 1995).

Among the various recording configurations that can be attained with the patch-clamp technique, i.e., cell-attached, excised-patch, and whole-cell, the last one is the most widely used, although it has a major limitation: the pipette itself. The pipette's tapered shank and small tip opening result in high access resistances and constitute the dominant barrier to molecular diffusion between pipette and cell cytosol (Pusch and Neher 1988). This shortcoming has the following consequences:

1. Errors in membrane potential control result due to the voltage drop across the access resistance in the presence of large membrane currents.

Special Issue: SIBPA 2011 Meeting.

M. Benedusi · M. Aquila · A. Milani · G. Rispoli (✉)
Dipartimento di Biologia ed Evoluzione, Sezione di Fisiologia e
Biofisica, Università di Ferrara, Via L. Borsari 46,
44100 Ferrara, Italy
e-mail: rsg@unife.it

- The precise measurement of current onset and offset kinetics is impeded due to the often too large time constant of charging the cell membrane capacitance through the access resistance.
- Intracellular ion accumulation or depletion results and slows down the rate of the incorporation of exogenous molecules via the patch pipette.

Another challenge with patch-clamp recording is to consistently achieve tight seals. Although the technique has been widely used for more than 40 years, little is still known about the nature of the molecular interactions underlying the generation of the seal between membrane and glass (the latest and most comprehensive studies: Priel et al. 2007; Suchyna et al. 2009). This lack of knowledge has given rise to all sorts of laboratory tales about how to prepare pipettes, solutions, and cells, resulting in a day-to-day variability in the ability to attain a seal (brilliantly described by Miller 2009) that has been a nightmare for two generations of scientists.

In this paper, the existing method has been improved by enabling the pipette shank to be enlarged (Goodman and Lockery 2000; Johnson et al. 2008) through the calibrated combination of heat and air pressure with a custom-made inexpensive set-up. These pressure-polished pipettes consistently gave access resistances that were one-quarter the size of the conventional ones, even using the most unfavorable cells, such as the isolated photoreceptor rod outer segment (OS) mechanically isolated from the frog retina. In addition to improving the electrical recordings, the pressure-polished pipettes minimized intracellular ion accumulation or depletion as well, allowing the fast cytosolic incorporation of exogenous molecules (as shown here by fluorescence imaging), especially via pulled quartz or plastic perfusion tubes. The latter could be positioned very close to the pipette tip, resulting in the intracellular incorporation of even large molecules such as proteins within a

few seconds (instead of >1 min as in the case of conventional pipettes) after they were expelled from the perfusion tube. Finally, a method is presented here that allows one to use conventional or pressure-polished pipettes made from just *one* glass type to consistently achieve seals on a wide variety of cell types, isolated from different amphibian, reptilian, fish, and mammalian tissues, and on artificial membranes made with many different lipid mixtures.

Methods

Pressure-polishing set-up

Patch pipettes were pulled in the conventional manner from 50 or 100 μl borosilicate glass microcaps (Drummond, Broomall, PA, USA), with a vertical puller (model PP-830, Narishige, Tokyo, Japan), and tightened into a pipette holder (Fig. 1, right). The latter was clamped to the microscope stage (Fig. 1), and a three-way valve allowed the pipette to be connected to a pressurized air line (set to ~ 4 atm and filtered to 0.2 μm to avoid pipette clogging) or to vent it to air.

The pipette holder was moved by means of the XY manipulator of the microscope stage to center the pipette tip into the central bend of an “omega”-shaped, glass-coated platinum filament (50 μm of diameter; Fig. 2). This shape ensured the homogeneous softening of the pipette shank when the filament was heated by passing a constant current through it and was obtained by using the needle of a 1 ml syringe and fine forceps. To avoid metal evaporation onto the pipette, the filament was uniformly glass-coated by dipping it in borosilicate glass powder heated to yellow color. The filament was tin-soldered to a copper holder (that also functioned as a heat sink; Fig. 2, top) mechanically coupled to a micromanipulator and electrically

Fig. 1 Set-up to fabricate the pressure-polished pipettes. *Left* View of the microscope, the camera coupled to the objective nosepiece, the microscope stage, the filament holder, the LED illuminator, and the box; *right* closer view of the microscope stage, the pressurized pipette holder, and the platinum filament

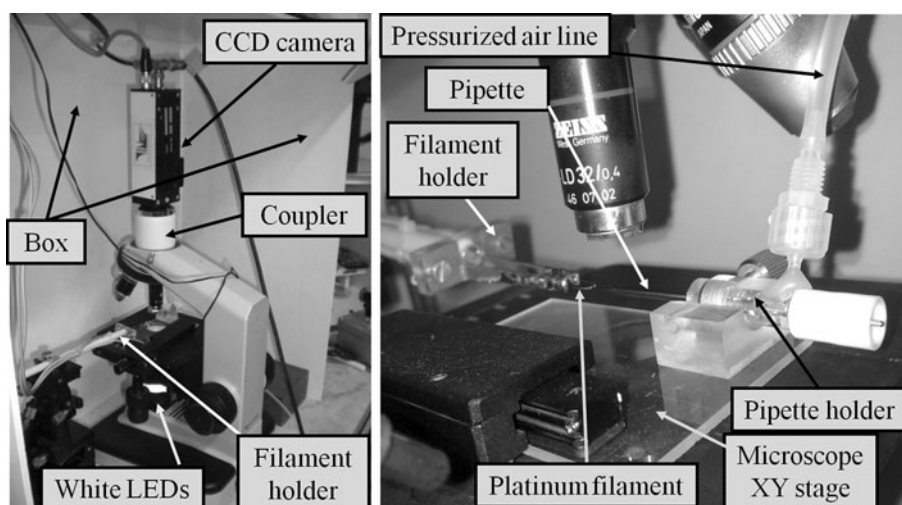
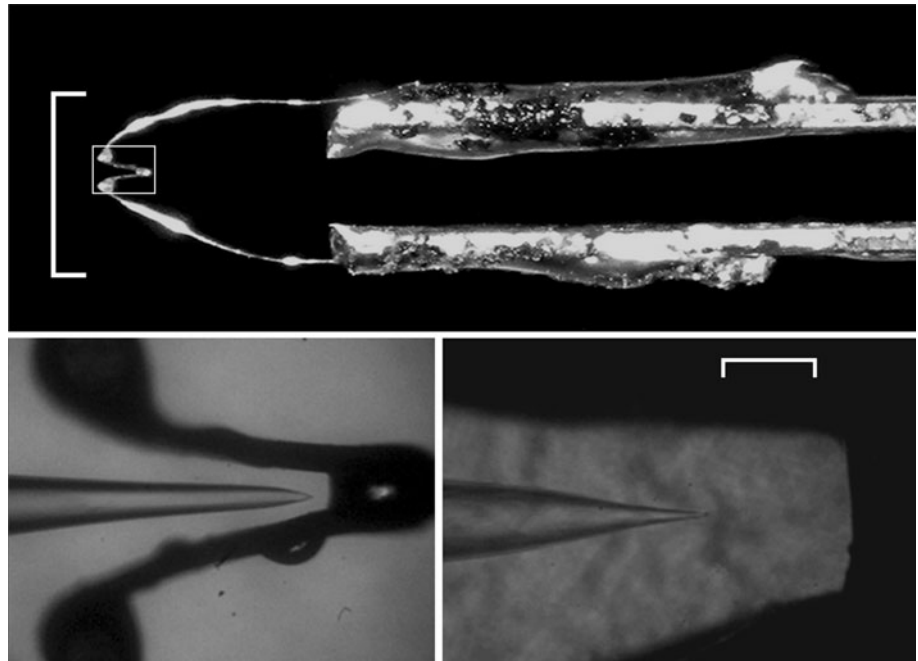


Fig. 2 Filament shape and pipette alignment. *Top* Shape of the glass-coated platinum filament tin-soldered to the holder; *scale bar* 5 mm. The region within the *white box* is enlarged at *bottom left*, where a pipette is shown properly aligned with the filament to ensure uniform pipette heating, at the end of a mild pressure polishing. The “omega”-shaped region of the filament is enlarged at *bottom right*, where a pipette is shown before pressure polishing, correctly aligned with the filament; *scale bar* 100 μ m



connected to a variable current generator. To produce adequate heat to soften the pipette tip (i.e., the filament was brought to reddish color), the current was typically set to ~ 1.2 A for filaments shaped as shown in Fig. 2 (at three different magnifications). The current generator was custom-made on the basis of the circuit reported in a web site (Regan 2005) and was remotely connected or not to the filament by a “push-to-make” switch.

The halogen lamp illuminator of the microscope was replaced with a custom-made light source using white LEDs (Fig. 1, left); a frosted filter and a regulated low-current generator were used to even out the light intensity in space and time. This light source was necessary to avoid the large amount of heat produced by the microscope’s built-in halogen lamp; the latter may increase the temperature (monitored with a digital thermometer) of the box containing the entire pressure-polishing set-up to the point of erratically affecting the fine control of the pipette temperature attained by the platinum filament. This box (which can be opened on the front to allow the pulled pipette to be loaded into and unloaded from the pipette holder) was necessary to protect the entire set-up from dust and the filament from air currents, which could also strongly affect the filament temperature; the push-to-make switch and the three-way valve were therefore positioned out of the box. The optical field containing the filament and the pipette was viewed on an LCD monitor connected to a contrast-intensified CCD camera (VX 44, Till Photonics, Gräfelfing, Germany) that replaced the objective turret of a bright-field stereomicroscope (YS2-T, Nikon, Tokyo, Japan; Fig. 1, left). The video signal was also digitized on-line (by

Pinnacle Studio MovieBox DV, Avid, Burlington, MA, USA) and stored on a computer to have a record of the time course of the pipette-shaping process. The video recordings were further processed off-line by using a commercially available program (Pinnacle Studio 9). The camera was coupled to the objective nosepiece (equipped with 10 \times , 20 \times , and long working distance 32 \times objectives) through an ocular, a 0.6 neutral density filter, and an infrared filter (all positioned in the custom-made optical “coupler”; Fig. 1, left). These two filters were necessary to cut the intense infrared light produced by the filament, which could saturate the camera; the pipette was viewed clearly by increasing the light intensity of the LEDs, which did not produce any infrared light.

Pipette fabrication and use

Once the pipette was properly aligned with the filament, the box was closed and the air pressure and the filament heating were turned on and off for an appropriate time (to attain the desired pipette shape), with the three-way valve and the push-to-make switch, respectively. The shaping process of the pipette shank and the tip was precisely followed using the calibration grating superimposed on the LCD monitor.

In order to have a very high rate of sealing on virtually *any* membrane surface, the pipette must be kept clean. Therefore, the microscope stage, the puller, and the pipette storage jar were carefully kept dirt-free, the pipette holder was frequently ultrasonicated in distilled water and ethanol (50:50 v/v), and the platinum filament was routinely

cleaned with ethanol. Moreover, the microcaps were thoroughly cleaned with ethanol, avoiding touching them with bare hands especially in their center, i.e., the area that will be thinned to form the pipette tips. To keep the pipette in the bath as little as possible, the microscope objective was focused first on the bottom of the chamber while the pipette was in the air, i.e., at the “home position” of the step motor micromanipulator (model 5171, Eppendorf, Hamburg, Germany) employed to move the head stage of the patch clamp amplifier (Axopatch 200B, Molecular Devices, Sunnyvale, CA, USA). The chamber was then moved away, the pipette was brought (while still in the air) a little above the focus of the chamber bottom, and these coordinates were stored in the micromanipulator memory. The pipette was then returned to the home position, and the chamber was brought back on the objective to search for the suitable membrane target. Finally, the pipette was returned to the previously memorized position, which was now just above the membrane target, while maintaining a strong positive pressure. Once the pipette was close to the target, the strong pressure was released, but a positive pressure was kept by mouth to clean the cellular debris from the membrane area where it was intended that the pipette would be sealed, while avoiding blowing the target away, especially if it was a small isolated cell. This “pressure cleaning” was not sufficient, however, to remove connective tissue or other organic material strongly adhering to the membrane target. When this was the case, it was necessary to use specific proteolytic enzymes, following known protocols described in detail in the literature.

Membrane targets employed

The conventional fire-polished or pressure-polished pipettes prepared with the borosilicate glass microcaps described above were able to attain tight seals on an extremely wide range of membrane substrates, such as sensory cells (labyrinthine hair cells, Martini et al. 2000; retinal rods and cones from reptilian, amphibian, and fish retinae, Rispoli 1998; Moriondo and Rispoli 2010; unpublished results), neurons (horizontal cells, bipolar cells, and ganglion cells enzymatically dissociated from turtle retinae, following the isolation protocol of Tatsukawa et al. 2005), culture cells (HEK 293, Navangione et al. 1997; NB4, Brugnoli et al. 2007; MDA-MB-231, Bertagnolo et al. 2007; COS and HeLa, unpublished results), muscle cells (cardiac myocytes enzymatically isolated from the excised hearts of rats using the protocol of Comini et al. 2005), and erythrocytes from amphibian (Rispoli et al. 2009), reptilian, fish, and human blood (unpublished results). These pipettes also sealed perfectly on giant unilamellar vesicles (GUVs), prepared by electroformation (Stella et al. 2007) using the following nine different lipid

compositions (also employing fluorescent-labeled lipids in order to check the GUV unilamellarity with fluorescence): egg phosphatidylcholine (ePC) 90%, egg phosphatidylglycerol (ePG) 10%; ePC 65%, ePG 10%, cholesterol (C) 25%; ePC 55%, ePG 10%, C 25%, nitrobenzoxadiazol-labeled phosphatidylethanolamine (NBD-PE) 10%; ePC 55%, ePG 10%, C 25%, dansyl-labeled phosphatidylethanolamine (dansyl-PE) 10%; ePC 40%, ePG 20%, C 30%, NBD-PE 10%; ePC 30%, ePG 10%, C 50%, NBD-PE 10%; dipalmitoylphosphatidylcholine (DPPC) 95%, NBD-PE 5%; DPPC 90%, ePG 5%, NBD-PE 5%.

All chemicals were purchased from Sigma Aldrich (St. Louis, MO, USA) except phospholipids, which were purchased from Avanti Polar Lipids (Alabaster, AL, USA). Animal experiments and care were in compliance with the Declaration of Helsinki guidelines, and a local ethics committee approved the experimental procedures.

Cell viewing, electrophysiological recording, and fluorescence imaging

An aliquot (~2 ml) of the appropriate Ringer solution containing the isolated cells (or tissue fragments, tissue slices, or GUVs) was transferred to the recording chamber placed on the microscope (TE 300, Nikon) stage. The preparation was illuminated with an ultrabright infrared LED (900 nm) and focused on a fast digital camera (C6790-81, Hamamatsu Photonics, Tokyo, Japan) coupled to the microscope. The preparation was then viewed in the frame grabber window generated by the AquaCosmos software package (version 2.5.3.0; Hamamatsu Photonics), which also controlled all the camera parameters (such as gain, frame rate, binning, etc.) via a PCI board (PCDIG, Dalsa, Waterloo, ON, Canada). In addition to bright-field viewing of the cells, the camera and the software were employed for fluorescence imaging experiments; the excitation light was generated by a monochromator (Polychrome II, Till Photonics) coupled to the epifluorescence port of the microscope via an optical fibre. The concentration of lucifer yellow (CH, dilithium salt) in the imaging experiments was 350 μM (excitation: 425 nm, emission: 528 nm).

Cells were recorded using the whole-cell configuration of the patch-clamp technique under visual control at room temperature (20–22°C) employing an Axopatch 200B; pipette and extracellular solutions were as reported in the literature, specified in the previous section for each cell system. The GUVs were recorded in excised-patch configuration in symmetric Na^+ or K^+ (130 mM) and Ca^{2+} (1–5 mM), buffered to pH = 7.6 with 10 mM HEPES free acid [*N*-(2-hydroxyethyl)piperazine-*N'*-(2-ethanesulfonic acid)] and NaOH (osmolality 260 mOsm/Kg). Recordings were filtered at 2 kHz via an eight-pole Butterworth filter

(VBF/8 Kemo, Beckenham, UK) and sampled on-line at 5 kHz by a Digidata 1322A (Molecular Devices) connected to the SCSI port of a Pentium computer running the pClamp 9.0 software package (Molecular Devices), and stored on disk. Data were analyzed using Clampfit (version 9.0; Molecular Devices); SigmaPlot (version 8.0; Jandel Scientific, San Rafael, CA, USA), AquaCosmos software package, and Photoshop CS4 (Adobe Systems, San Jose, CA, USA) were used for figures and statistics. Results are given as means \pm SEM.

Results and discussion

Pressure-polishing procedure

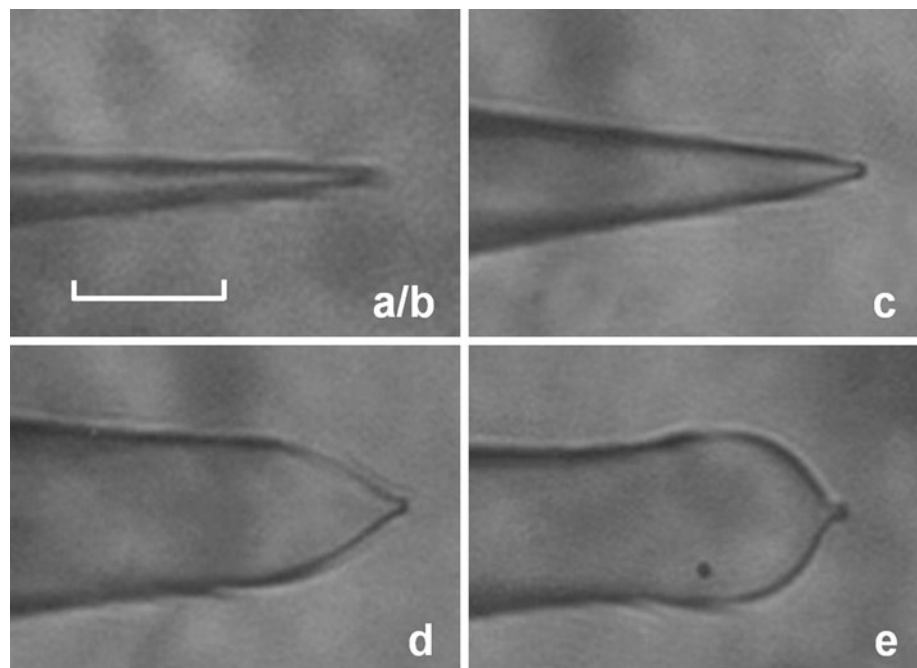
The pipette shank geometry and its tip opening diameter could be finely controlled by adjusting: (1) the relative position of the pipette with respect to the filament, (2) the current intensity passing through the filament, (3) the duration of the current flow, (4) the pressure intensity, and (5) the duration of the pressure application while the current was flowing in the filament. In order to standardize the technique, the most efficient strategy found was to optimize parameters (1), (2), and (4) and to keep them fixed throughout the pressure-polishing process, while parameters (3) and (5) were left to be adjusted each time in order to obtain the desired shank profile and tip opening diameter. Long pressure applications (while the current was flowing in the filament) were used to obtain very enlarged shanks. If the pipette opening was too large for a given

pressure duration, then its tip was heated again in the absence of pressure until the desired size was achieved; if it was too small, then that pressure duration was applied to pipettes pulled with larger tips. With the set-up built as detailed in the “Methods” section, any undergraduate student, with a few hours of practice, was able to quickly and reproducibly fabricate pipettes with an arbitrary shank profile and tip opening diameter.

To provide a quantitative measure of the performances of the pressure-polished pipettes, the bubble number of pulled pipettes (Fig. 3a) and the bubble number, ohmic resistance, and access resistance (measured on the frog OS recorded in whole cell; Fig. 4a–d; Rispoli 1998) of the pulled pipettes were measured after polishing them with (Fig. 3c–e) or without (Fig. 3b) pressure, for four different representative geometries (Fig. 3b–e; Table 1). The pipettes of Fig. 3 were tested on frog OS because this was the most critical cell system among those tested (reported in “Methods”). Indeed, to have reliable recordings from frog OS, it was necessary to use pipettes with a very small tip diameter (which would have yielded high access resistances if fabricated with conventional methods) to avoid breaking the OS, because they were very fragile, had a small diameter (Fig. 4a, c), and were often soiled with retina debris and vitreous humor.

The conventional fire polishing reduced the tip opening diameter of the pulled pipette (see column “ BN_f ” of Table 1; $n = 15$ for all pipette geometries) without affecting the shank profile (Fig. 3b), resulting therefore in increased pipette resistance once filled with saline solution (and placed in the bath; see column “ R_p ” of Table 1). The

Fig. 3a–e Different pipette shanks obtained with the pressure fire polishing. **a** Pulled pipette; **b** the same pipette fire polished without pressure (indistinguishable from the pulled one at this magnification); **c–e** pulled pipettes similar to **a**, fire polished with progressively longer pressure durations. Scale bar 20 μ m



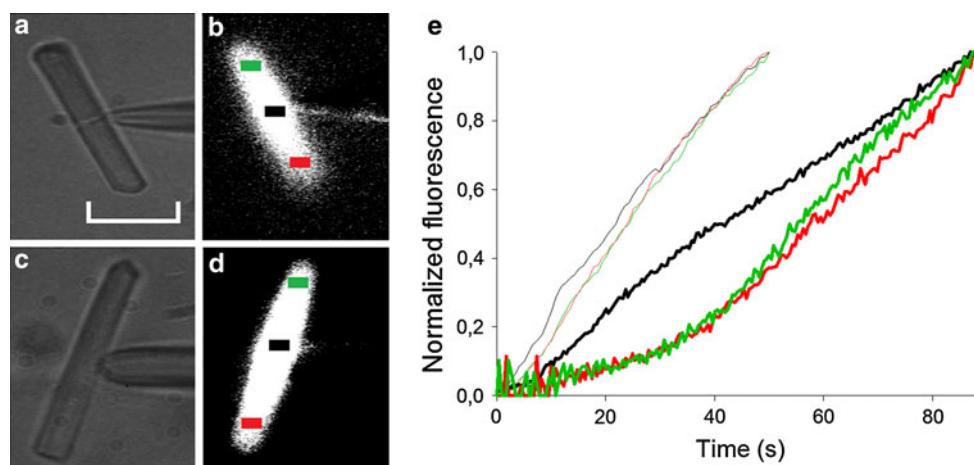


Fig. 4a–e Kinetics of a lucifer yellow loading into a frog OS recorded in whole cell for two different pipette geometries. **a, c** Bright-field images of a whole-cell configuration recording with **a** a conventional fire-polished pipette (shown in **b** in fluorescence; access resistance $\sim 24 \text{ M}\Omega$) and **c** a pressure-polished pipette (shown in **d** in fluorescence; access resistance $\sim 7 \text{ M}\Omega$), respectively. Scale bar $20 \mu\text{m}$. **e** Normalized fluorescence intensity integrated over the *black*, *green*, and *red* regions versus time for the fluorescence imaging

recording in **b** (*thick* traces) and **d** (*thin* traces). The normalized fluorescence, integrated over the *black* region, reached about 50% of the maximum at 40.9 s in **b** (data from **e**, *black thick* trace) and at 21.8 s in **d** (**e**, *black thin* trace); the integrated fluorescence in *green* and *red* regions was 0.24 and 0.23, respectively, at 40.9 s in **b** (**e**, *green* and *red thick* traces) and 0.45 in both regions at 21.8 s in **d** (**e**, *green* and *red thin* traces)

Table 1 Quantitative parameters of the patch pipettes

Geometry	BN_i	BN_f	R_p (M Ω)	R_a (M Ω)
a	5.3 ± 0.1	–	5.6 ± 0.7	–
b	5.5 ± 0.2	4.8 ± 0.2	7.0 ± 0.7	26.4 ± 0.8
c	5.8 ± 0.2	5.1 ± 0.1	3.2 ± 0.5	22.7 ± 2.6
d	5.8 ± 0.2	5.0 ± 0.2	2.3 ± 0.2	10 ± 2
e	5.6 ± 0.3	5.1 ± 0.1	2.4 ± 0.2	6.5 ± 1.3

BN_i Initial bubble number after pulling the pipette, BN_f final bubble number of the polished pipette (with or without pressure application), R_p pipette resistance in the bath, R_a access resistance, $n = 15$

fire polishing significantly increased the probability of achieving a seal on all cells tested, although the access resistance was high, especially for the pipette employed for frog OS recordings (Table 1). Many authors have suggested (Penner 1995) that conventional fire polishing improves the sealing capacity of the pipette by removing any contaminants left on the tip after coating with insulating agent to reduce capacitance between the pipette interior and the bath. This would not be true in this case because no coating was used in these experiments and, if the protocols as described in the “Methods” section were followed, the pipette should already be perfectly clean. Instead, the fire polishing thickened the wall and smoothed the surface of the pipette tip, which is expected to be quite rough (at the molecular level) after it is abruptly separated from its companion following the pulling procedure. It is conceivable that a larger membrane surface could seal on the glass surface that was smoother and thicker than the

rough and thin one of the pipette just pulled, resulting in an increase in the seal resistance. This view is also supported by the following observation: occasionally, when a large bleb was formed after a seal was achieved (in the $G\Omega$ range) with pipettes or cells that were not perfectly clean or with pipettes that were not fire polished, most of this bleb could be expelled out of the pipette by applying a positive pressure without any change in the seal resistance. This indicates that the portion of the glass tip that sealed on the membrane and the membrane itself formed very stable assemblages around which the lipids that did not seal on the glass could flow quite freely. If the seal was instead very good (seal resistance $>20 \text{ G}\Omega$)—that is when fire-polished pipettes unsoiled by bath debris were used and on clean cell surfaces, and therefore a much larger glass surface sealed on the membrane—it was not usually possible to eject the bleb unless the applied pressure inside the pipette was so large as to break the seal.

By carefully regulating the duration of pressure and the application of heating, the pipette shank was widened as desired, while the tip opening diameter could be increased, decreased, or left unchanged, resulting in a fourfold reduction of access resistance for pipettes as shown in Fig. 3e with respect to the conventional ones (Fig. 3b; Table 1). As expected, for a fixed shank geometry, as the pipette tip opening was made larger, the bubble number increased, while the pipette and access resistance decreased. However, pressure-polished pipettes with similar bubble number and resistance (Table 1), but with very different shanks and tip openings, gave quite different

access resistances. Therefore, to reproduce a desired pipette geometry, it was necessary to rely on the bubble number of the pulled pipette (which was always fabricated with the same shank) and on the pressure-polishing parameters (i.e., heating and pressure durations), rather than on the bubble number of the polished pipette only.

Sealing on virtually any membrane with just one glass type

Surprisingly, the chosen borosilicate glass (see “Methods”) was extremely good at attaining tight seals on an extremely wide variety of cells, in isolation or inserted in small tissue fragments or slices, or on giant unilamellar vesicles (GUVs) of many different lipid composition (see “Methods”). Therefore, it was not true, as commonly believed, that different types of glass work better on different cell types (Penner 1995). Moreover, in contrast to the literature (Coronado 1985), it was possible to routinely gain seals exceeding 10 G Ω with GUVs of up to 90% phosphatidylcholine. Therefore, when there was a failure to achieve a seal, it was because the patch pipette tip was soiled and/or because the membrane target was contaminated with cell debris, connective tissue, or other organic material, not because the glass type was inappropriate. The day-to-day variability in attaining the seal was therefore entirely due to the cell quality (soiled or too fragile to sustain the sealing process), not to some uncontrollable parameter in the pipette fabrication. Indeed, if the protocol described in “Methods” was strictly followed—i.e., the pressure-polishing set-up was maintained dirt-free, the pipette was kept in the bath as little as possible (to avoid cell debris soiling the tip while approaching the cell), and the membrane target was “pressure cleaned”—the seal was guaranteed. Moreover, it was sometimes possible to achieve a seal with the same pipette more than once, especially when the cell’s extracellular matrix was broken down with enzymatic treatment (Corey and Stevens 1983), allowing us to move as quickly as possible from one cell to the other, to avoid soiling the pipette. Although the seal resistance consistently decreased from one trial to the next, it was possible to have seal resistances above 1 G Ω up to the fourth consecutive seal with the *same* pipette. To confirm that the lack of seal was not due to the pipette (if properly fabricated) but to the cell quality, it was observed many times on enzyme-treated or cultured cells that, if the first seal attempt was unsuccessful, it was still possible to achieve a seal with the *same* pipette on another cell. Finally, in contrast to what has been reported by many authors, but in agreement with Priel et al. (2007), it was found that at physiological pH, the presence or absence of Ca²⁺ in the patch pipette was not necessary to promote the seal. Indeed, it was possible to routinely achieve a seal with the

patch pipette filled with solutions containing up to 30 mM BAPTA or 30 mM Ca²⁺ (see also Rispoli 1998; Rispoli et al. 1995). In the latter case, it was obviously not possible to attain the whole-cell recording because cells immediately underwent apoptosis; a whole-cell recording could be achieved in the OS, however, since they are not endowed with Ca²⁺-dependent proteases.

Given the “sealing power” of the glass pipette mentioned above, the pressure-polishing technique was optimized just for this glass type.

Intracellular perfusion

In addition to the dramatic improvements in electrical recordings, the pressure-polished pipettes also increased the rate of molecular diffusion between the pipette and the cell interior, as shown by the time course of fluorescence dye loading of the frog OS cytosol via the patch pipette. In this experiment, illustrated in Fig. 4, the rate of the fluorescence (Fig. 4e), integrated over three OS cytoplasmic rectangular regions of the same area positioned at the level of the patch pipette and at the two OS ends (Fig. 4b, d), increased with time. One experiment (Fig. 4a, b, e, thick traces) was carried out with a conventional patch pipette (Fig. 3b), the other one (Fig. 4c, d, e, thin traces) with a pressure-polished pipette with a geometry in between the ones illustrated in Fig. 3c and e. To avoid errors due to saturation of the camera at the end of the whole-cell recording (when the fluorescence inside the cell was intense), while also maintaining a good sensitivity at the beginning (when fluorescence was scarce, especially in the case of conventional patch pipettes), the following strategy was adopted. Once a particular gain of the camera was set (that was necessarily high in the case of conventional pipettes), the fluorescence was followed (at a rate of 5 frames/s) in the whole-cell configuration (corresponding to zero time in Fig. 4e) until it reached about 50% of the maximum light intensity detected by the camera. The integrated fluorescence in each one of the six rectangular regions of Fig. 4 was then normalized to the latter fluorescence intensity. Before normalization, the two fluorescence images, acquired during cell-attached recording in the two experimental conditions of Fig. 4 just before breakthrough, were subtracted from the corresponding image stack recorded in the whole-cell configuration in order to correct all images for the pipette fluorescence and possible cell autofluorescence (two corrected images, acquired when fluorescence was 80% of the maximum, are shown in Fig. 4b, d). The rate of lucifer yellow concentration increase in the cytosol obtained with the pressure-polished pipettes (Fig. 4e, thin traces) was about twofold (1.8 ± 0.4 , $n = 4$) faster than with conventional pipettes (Fig. 4e, thick traces). This larger concentration rise at the

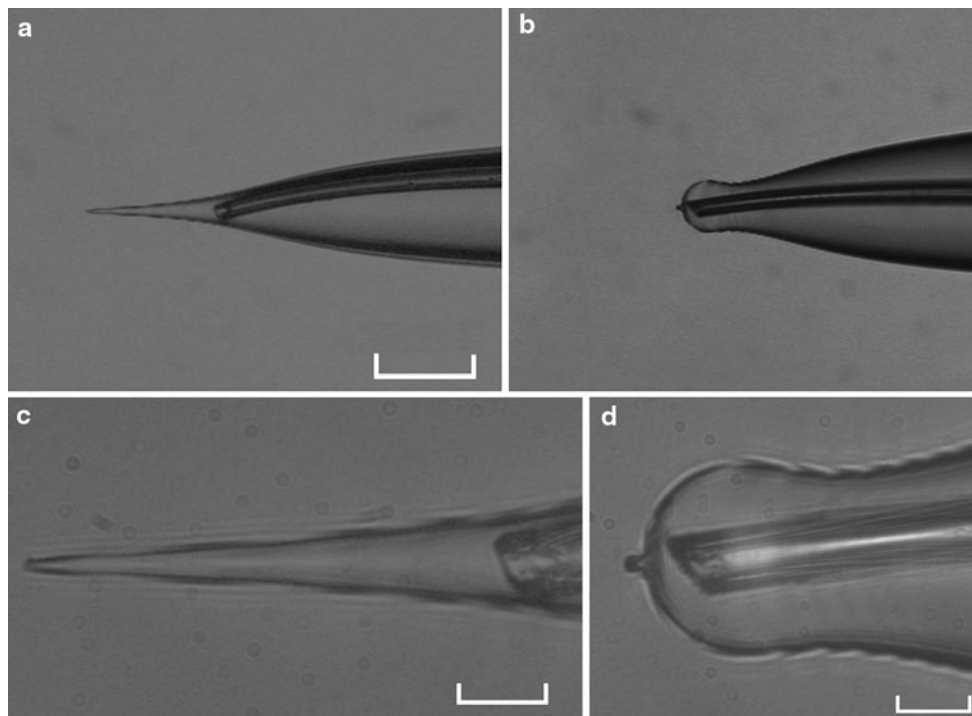


Fig. 5a–d Controlled intracellular perfusion. **a** A pulled quartz tube is positioned inside the lumen of a conventional pipette as close as possible to its tip, magnified in **c**; **b** the same tube is inserted in a

pressure-polished pipette, magnified in **d**. Scale bar 100 μm in **a** and **b**, and 20 μm in **c** and **d**

level of the patch pipette (black traces) also produced a faster longitudinal diffusion toward the two OS ends (although the presence of the disk stack should hinder this diffusion) than the conventional pipettes as indicated by the shorter delay between the rate of fluorescence increase at these two OS ends (red and green traces) with respect to the one at the level of the patch pipette (black trace).

The substantial improvement in cell dialysis achieved by the pressure-polished pipettes allows small proteins and peptides in the cytosol to perfuse, enabling the “real time modulation” of a multitude of cellular processes, such as the signal transduction cascades. However, proteogenic molecules stick to the glass tip, preventing seal formation, therefore it is important to add them to the pipette solution to a later time, i.e., after the seal has been achieved. In general, it is important to apply a particular molecule under test to the cytosol, not at the beginning of the whole-cell recording, but at a desired later time. This goal can be realized by inserting pulled quartz tubes in the pipette lumen (or tubes fabricated with plastics that can be easily softened with a Bunsen flame, such as polyethylene or polypropylene), filled with a solution containing the molecule under test. The latter can be ejected into the pipette solution with a pulse of pressure applied to the tube lumen. These tubes can be inserted very close to the tip of pipettes with a particularly enlarged shank (i.e., very close to the cell cytosol; Fig. 5), therefore the molecule under test is

applied to the cell cytosol with a very short delay with respect to the time with which they were expelled out of the perfusion tube. Indeed, the enlarged pipette shank (Fig. 5b, d) allowed the smallest quartz perfusion tube that could be handled ($\sim 10 \mu\text{m}$ internal diameter and $\sim 18 \mu\text{m}$ external) to advance $x = 95 \mu\text{m}$ further than the conventional pipette shank (Fig. 5a, c), reducing the perfusion delay for a small protein (with a diffusion coefficient $D = 10^{-6} \text{ cm}^2 \text{ s}^{-1}$) by about 15 s, according to the three-dimensional diffusion equation in the absence of pressure:

$$t = \frac{x^2}{6 \cdot D}$$

However, pulled quartz tubes with such a small diameter are extremely fragile and difficult to handle. More robust tubes with an external diameter up to $\sim 45 \mu\text{m}$ were positioned inside an enlarged shank pipette as close to the pipette tip as the above one (Fig. 5d), but they had to be positioned as far as $\sim 200 \mu\text{m}$ from the pipette tip in the case of conventional pipettes, resulting in a perfusion delay of $\sim 70 \text{ s}$.

Acknowledgments We thank Dr. Lorenzo Stella, University of Rome Tor Vergata, Italy, for preparing the GUVs and teaching us the GUV electroformation technique; Dr. Antonella Boraso for providing cardiac myocytes enzymatically isolated from the excised heart of rats; Anna Fasoli for helping in the preparation of many experiments; and Andrea Margutti for technical assistance. Federica Baldassari, Anna Fasoli, Cristina Mantovani, and Arua Sibahi helped build the

pressure-polishing set-up and fabricate the patch pipettes. Financial support to G.R. included grants from the Ministero dell'Università e della Ricerca (MIUR), Roma (Italy; Project PRIN 2008), from the "Comitato dei sostenitori dell'Università di Ferrara" (Italy; Project FAR 2009 and 2010), and from Fondazione Cassa di Risparmio di Cento.

Conflict of interest The experiments comply with the current laws of Italy; the authors declare that they have no conflict of interest.

References

- Bertagnolo V, Benedusi M, Brugnoli F, Lanuti P, Marchisio M, Querzoli P, Capitani S (2007) Phospholipase C-beta 2 promotes mitosis and migration of human breast cancer-derived cells. *Carcinogenesis* 28:1638–1645
- Brugnoli F, Bavelloni A, Benedusi M, Capitani S, Bertagnolo V (2007) PLC-beta2 activity on actin-associated polyphosphoinositides promotes migration of differentiating tumoral myeloid precursors. *Cell Signal* 19:1701–1712
- Comini L, Boraso A, Bachetti T, Bernocchi P, Pasini E, Bastianon D, Curello S, Terracciano CM, Ceconi C, Ferrari R (2005) Effects of endotoxic shock on neuronal NOS and calcium transients in rat cardiac myocytes. *Pharmacol Res* 51:409–417
- Corey D, Stevens C (1983) Science, and technology of patch recording electrodes. In: Sakmann B, Neher E (eds) *Single-channel recording*, 1st ed. Plenum Press, New York, pp 53–68
- Coronado R (1985) Effect of divalent cations on the assembly of neutral and charged phospholipid bilayers in patch-recording pipettes. *Biophys J* 47:851–857
- Goodman MB, Lockery SR (2000) Pressure polishing: a method for re-shaping patch pipettes during fire polishing. *J Neurosci Methods* 100:13–15
- Johnson BE, Brown AL, Goodman MB (2008) Pressure-polishing pipettes for improved patch-clamp recording. *J Vis Exp*. doi:10.3791/964
- Martini M, Rossi ML, Rubbini G, Rispoli G (2000) Calcium currents in hair cells isolated from semicircular canals of the frog. *Biophys J* 78(3):1240–1254
- Miller C (2009) Everything you always wanted to know about Sachs' seals. *Biophys J* 97:687
- Moriondo A, Rispoli G (2010) The contribution of cationic conductances to the potential of rod photoreceptors. *Eur Biophys J* 39:889–902
- Navangione A, Rispoli G, Gabellini N, Carafoli E (1997) Electrophysiological characterization of ionic transport by the retinal photoreceptor exchanger expressed in HEK293 cells. *Biophys J* 73:45–51
- Penner R (1995) A practical guide to patch clamping. In: Sakmann B, Neher E (eds) *Single-channel recording*, 2nd ed. Plenum Press, New York, pp 3–30
- Priel A, Gil Z, Moy VT, Magleby KL, Silberberg SD (2007) Ionic requirements for membrane-glass adhesion and giga seal formation in patch-clamp recording. *Biophys J* 92:3893–3900
- Pusch M, Neher E (1988) Rates of diffusional exchange between small cells and a measuring patch pipette. *Pflugers Arch* 411:204–211
- Regan T (2005) Current sense circuit collection. Making sense of current. Application note 105, current control. http://www.linear.com/ad/19-current_control.pdf
- Rispoli G (1998) Calcium regulation of phototransduction in vertebrate rod outer segments. *J Photochem Photobiol B* 44:1–20
- Rispoli G, Navangione A, Vellani V (1995) Transport of K⁺ by photoreceptor Na⁺-Ca²⁺, K⁺ exchanger in isolated rods of lizard retina. *Biophys J* 69:74–83
- Rispoli G, Milani A, Infanti M, Benedusi M, Aquila M, Vedovato N (2009) Pore forming properties of antimicrobial peptides in different natural lipid environment. *Biophys J* 96:535a
- Sakmann B, Neher E (1995) *Single channel recording*. Plenum Press, New York
- Stella L, Pallottini V, Moreno S, Leoni S, De Maria F, Turella P, Federici G, Fabrini R, Dawood KF, Bello ML, Pedersen JZ, Ricci G (2007) Electrostatic association of glutathione transferase to the nuclear membrane. Evidence of an enzyme defense barrier at the nuclear envelope. *J Biol Chem* 282:6372–6379
- Suchyna TM, Markin VS, Sachs F (2009) Biophysics and structure of the patch and the gigaseal. *Biophys J* 97:738–747
- Tatsukawa T, Hirasawa H, Kaneko A, Kaneda M (2005) GABA-mediated component in the feedback response of turtle retinal cones. *Vis Neurosci* 22:317–324